Vol. 84 No. 6 pp. 1488–1499 ACTA GEOLOGICA SINICA (English Edition) Dec. 2010

LA-ICP-MS Zircon U-Pb Geochronology and Petrology of the Muchang Alkali Granite, Zhenkang County, Western Yunnan Province, China

YE Lin[1, *], GAO Wei[1, 2], CHENG Zengtao[1, 2], YANG Yulong[1, 2] and TAO Yan[1]

1 *State Key Laboratory of Ore Deposit Geochemistry, Institute of Geochemistry, Chinese Academy of Sciences, Guiyang 550002, China*

2 *Graduate School of Chinese Academy of Sciences, Beijing 100049, China*

Abstract: The Muchang composite intrusion is located about 14 km southeast of the Fengwei town and south of the Baoshan-Zhenkang block. The rift-related intrusion consists of the early-stage riebeckite nordmarkite in the east and west sides and the discontinuous marginal zone, the late-stage main body of dominant riebeckite granite, and minor aegirine granite. Studies on petrological geochemistry and LA-ICP-MS zircon U-Pb dating of the late-stage riebeckite granite, origin and evolution of the Muchang alkali granite and the relationship between the granite and the associated skarn-type Luziyuan Pb-Zn deposit are discussed in this paper. The results show that the Muchang alkali granites belong to A-type granites, which are characterized by enrichment in Al_2O_3, SiO_2, total alkali and Fe, depletion in MgO and CaO contents with high FeO_T/MgO ratios. The REE concentrations are relatively high, exhibiting highly fractionated LREE patterns with significantly Eu negative anomaly. The Muchang granites are obviously enriched in lithophile elements (e.g., Rb, K, U and Th) and high field strength elements (e.g., Zr, Hf, Nb, Y and Ga) with high 10000×Ga/Al ratios and depleted in Sr, Ba, Ti, Cr and Ni, which are similar to those of the A-type granites and quite different from those of S-type and I-type granites. The LA-ICP-MS zircon dating results of the Muchang granite gave a weighted mean age of 266.2±5.4 Ma (2σ), suggesting that they were formed in the stage of extension at the end of post-collision at Middle Permian and the consumption of Paleo-Tethys ocean took place before 266 Ma. It is suggested that the unexposed intermediate-acid intrusive rocks in the Luziyuan ore district, which is the "sister" rocks material of the Muchang granites and related closely to Luziyuan Pb-Zn mineralization, were the product of Middle Permian.

Keywords: A-type granite, U-Pb age, Muchang alkali granite, tectonic setting, evolution of Tethys in southern Sanjiang area

1 Introduction

"A-type" granites occur in post-orogenic or intraplate tectonic settings (Eby, 1990, 1992; Black and Liegeois, 1993) and can provide significant information on post-collisional/intraplate extensional magmatic processes within the continental lithosphere and their contribution to the build-up of the upper continental crust (Turner et al., 1992; Mushkin et al., 2003), which have been the focus of numerous petrological studies. Loiselle and Wones (1979) described A-type granites to be generated along continental rift zones (anorogenic) and have mildly alkaline and less water. Recently, the meaning of concept of "A-type" granite has been enlarged more, e.g., the type of rocks including not only alkali granite but also calc-alkaline, metalkali-metaluminous, weakly peraluminous granites and the tectonic settings including post-orogenic setting and post-collision extensional settings (Whale et al., 1987; Eby, 1990; Wu et al., 2002; Martin, 2006; Shellnutt and Zhou, 2007; Bonin, 2007). Although there is no uniform concept of "A-type" granite and many argues about its definition, feature of source rock and origin (Skjerlie and Johnston, 1993; Wickham et al., 1996; King et al., 1997; Mingram et al., 2000; Litvinovsky et al., 2002; Mushkin et al., 2003). This kind of rocks are characterized by high Si and alkaline contents, low Mg and Ca contents, enrichment of HFSE (Nb, Zr, Y and Ga) and depletion of Sr and Ba, abnormally high ΣREE concentrations and typically

* Corresponding author. E-mail: yelin@vip.gyig.ac.cn

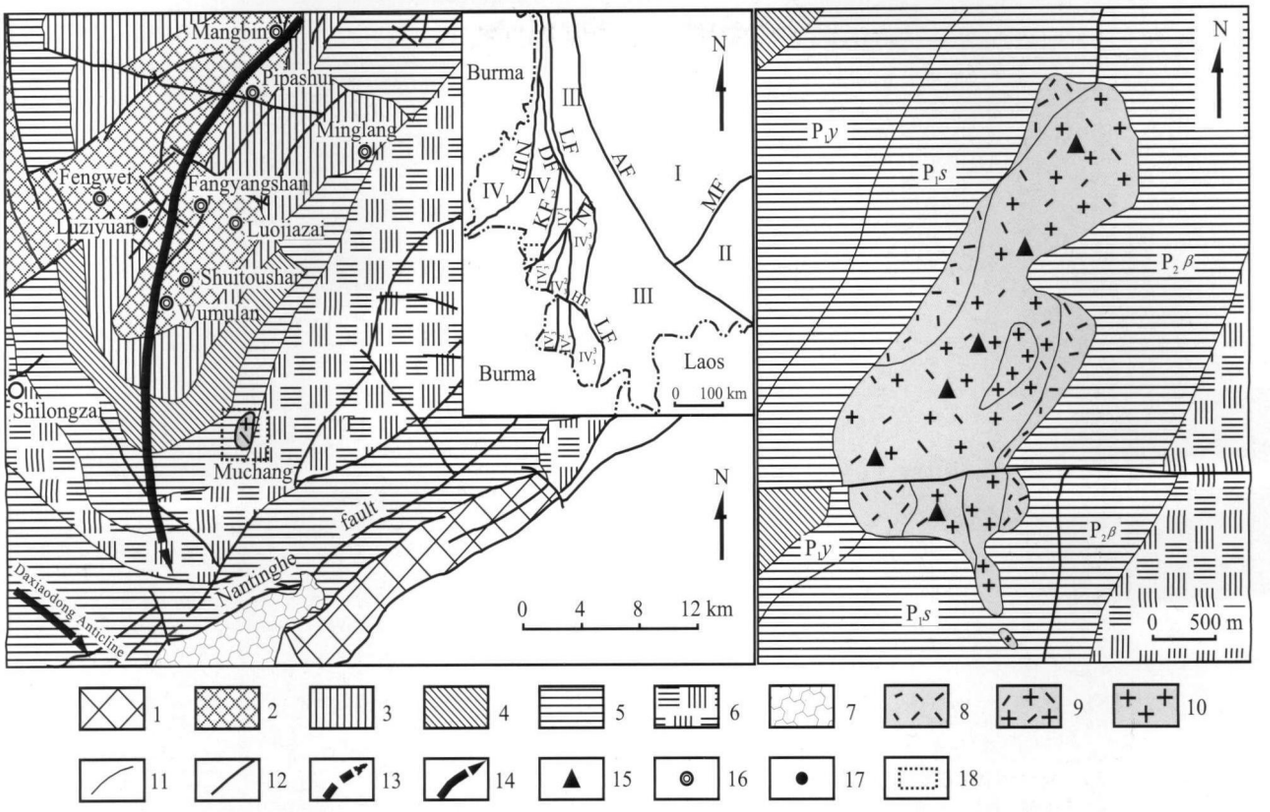

Fig. 1. Geological map of the Muchang alkali granite, Zhenkang, Yunnan Province (Modified from Gu et al., 1988 and Yunnan Bureau of Geological Survey, 2006).

1, late Proterozoic slate, phyllite and schist with limestone; 2, Cambrian clastic rocks and carbonate rocks; 3, Ordovician-Devonian sandstone, siltstone and dolostones; 4, carbonic metamorphic siltstone, phyllite slate, basalt, silty sandstone and limestone; 5, Permian limestone, dolostones with minor sandstone, shale and carbonaceous shale; 6, Triassic sandstone, limestone, dolostones and acidic volcanic rocks; 7, Quaternary proluvial sandy conglomerate and sandy clay; 8, riebeckit nordmarkite; 9, riebeckite granite; 10, aegirine granite; 11, stratigraphic boundary; 12, fault; 13, synclinal axis; 14, anticlinal axis; 15, sampling location; 16, city (village); 17, Luziyuan Pb-Zn deposit; 18, study area. I, Yangtze para-platform; II, South China fold system; III, Tanggula-Changdu-Lanping-Simao fold system; IV, Gangdisi-Nianqingtanggula fold system; IV_1, Bosulaling-Gaoligongshan fold system; IV_2, Fugong-Zhengkang fold belt; IV_3, Changning-Menglian fold belt; IV_3^1, Mengtong-Nanla-Ximeng fold belt; IV_3^2, Mengsheng-Donghui fold belt; IV_3^3, Lincang-Menghai fold belt; AF, Ailaoshan fault; LF, Lancangjiang fault; DF, Damangguangfang fault; KF, Kejie fault; NJF, Nujiang fault; HF, Heihe fault; NF, Nandinghe fault; MF, Mile-Shizong fault; $P_2\beta$, upper Permian volcanic rock series; P_1s, lower Permian Shazipo Formation limestone and dolomitic limestone; P_1y, lower Permian Yongde Formation argillaceous limestone with clastic rock.

LREE-enriched distribution patterns.

As one of an important part of east Tethys tectonic belt, numerous geological and geochemical studies focus on the relationship between tectonic setting and the evolution of Tethys tectonic belt in western Yunnan Province, China (Wang, 1996; Zhong, 1998; Pan et al., 2003; Wang et al., 2009; He et al., 2009; Deng et al., 2010). Geochemical and petrological studies on the giant S-type Linchang granites batholith (e.g., Lincang and Pinghejie) exposed in this region have provided valuable information about the tectonic evolution and metallogenesis in the Tethys of the Sanjiang area, southwestern China (Chen, 1987; Liu et al., 1989; Mo et al., 1998; Qin, 1999; Yu et al., 2003; Zhang et al., 2006; Peng et al., 2006; Yao et al., 2009; Fan et al., 2009). Due to the lack of systematic and precise ages for this region, different arguments for the timing of continent-continent collision or continent-arc collision during the evolution of Proto-Tethys were presented.

The Muchang alkali granite is located at southern Baoshan-Zhenkang block of Eastern Tethys tectonic belt. Although the largest exposed area is only 4.5 km^2, the origin of these rocks is important to understand the history of the evolution of Tethys tectonic belt. Furthermore, the Baoshan-Zhenkang block is one of the most important parts of southern section of "Sanjiang" metallogenic. The Baoshan-Zhenkang Pb-Zn polymetallic metallogenic belt was discovered in recent ten years, of which the large Luziyuan Pb-Zn polymetallic tectonic-skarn-bound deposit hosted in late Cambrian carbonate strata in the south block (Deng, 1995; Zhao et al., 2002; Xia et al., 2005; Dong, 2007; Dong and Chen, 2007), and the large Hetaoping Pb-Zn polymetallic deposit of same type in the north block (Chen et al., 2005; Zhu et al., 2006). Most of the studies indicated that this kind of mineralization is related to unexposed intermediate-acid granites (Zhao et al., 2002; Xia et al., 2005; Zhu et al., 2006; Dong, 2007; Dong and Chen, 2007). The Muchang alkali granite, located at south-east of the Luziyuan ore district, was suggested to be the "sister" rock material of the unexposed granites which host the Luziyuan Pb-Zn deposit in depth (Zhao et al.,2002; Dong, 2007; Dong and Chen, 2007). Thus, the study on the Muchang alkali granite is helpful to understand the Pb-Zn

Table 1 Major (wt%), trace (ppm) element concentrations of the Muchang granite

	MC08-01	MC08-02	MC08-03	MC08-04	MC08-05	A-type of world* (148)	A-type of China* (197)
SiO_2	76.77	75.57	76.46	74.12	71.57	73.81	73.55
TiO_2	0.29	0.25	0.41	0.37	0.57	0.26	0.23
Al_2O_3	13.00	13.21	13.34	14.35	15.48	12.40	12.81
TFeO	2.86	3.20	2.70	3.10	3.80	2.82	2.60
MnO	0.10	0.12	0.16	0.19	0.19	0.06	0.09
MgO	0.03	0.24	0.58	0.02	0.26	0.20	0.27
CaO	trace	0.42	0.09	0.06	0.55	0.75	0.82
Na_2O	1.93	2.07	2.26	2.54	3.15	4.07	3.76
K_2O	4.83	4.43	4.28	5.23	5.32	4.65	4.69
P_2O_5	0.03	0.04	0.07	0.04	0.09	0.04	0.07
LOI	0.99	0.87	1.07	0.67	0.62		
Total	100.84	100.41	101.42	100.70	101.61		
A/CNK	1.55	1.48	1.57	1.44	1.30	0.95	1.00
R1	3224.00	3192.00	3200.00	2721.00	2270.00	2331.00	2426.00
R2	257.00	318.00	299.00	289.00	373.00	337.00	357.00
A/MF	3.49	2.81	2.71	3.58	2.81	3.02	3.20
C/MF	0.00	0.16	0.03	0.03	0.18	0.33	0.37
AR	3.17	1.87	2.02	2.09	2.29	4.94	4.26
Differentiation Index	91.81	89.15	89.98	91.43	88.64	93.58	92.15
Ba	31.60	47.40	98.20	34.80	204.00	352.00	236.00
Rb	305.00	275.00	149.00	250.00	227.00	169.00	270.00
Sr	4.88	12.70	13.10	8.32	26.70	48.00	57.50
Ta	9.68	15.60	5.40	7.31	6.45		
Nb	133.00	165.00	83.90	132.00	104.00	37.00	34.90
Hf	23.10	27.90	14.50	22.00	15.50		
Zr	845.00	667.00	5950	819.00	583.00	528.00	334.00
Th	36.10	65.40	16.50	31.70	22.10		
U	10.80	18.30	5.52	8.36	8.82		
Cr	22.90	29.70	40.80	32.40	20.40		
Ni	8.35	9.04	11.40	8.83	10.00		
Sc	3.63	3.14	4.75	4.18	4.71		
V	2.27	3.67	7.11	2.40	3.73		
Pb	28.50	28.50	2.82	11.80	13.00		
Li	22.70	3.11	1.78	21.00	21.80		
Co	1.68	1.57	1.89	1.86	1.67		
Ga	28.80	30.20	23.60	29.10	28.80	24.60	18.54
Be	4.54	11.10	1.90	4.62	6.04		
Cu	2.29	2.87	3.43	3.66	3.60		
Zn	82.10	109.00	37.10	80.50	91.50		
Ge	1.75	1.38	1.38	1.70	1.80		
Y	71.60	110.00	35.80	71.40	65.50	75.00	54.03
La	112.00	76.00	35.40	108.00	92.30		
Ce	203.00	141.00	84.20	190.00	161.00		
Pr	22.40	18.60	8.27	24.00	20.00		
Nd	75.40	67.00	30.50	85.10	72.80		
Sm	13.00	16.20	6.23	16.70	14.00		
Eu	0.69	1.14	0.70	0.93	1.59		
Gd	11.30	14.30	5.25	13.10	11.90		
Tb	2.18	3.28	1.07	2.55	2.29		
Dy	13.00	19.80	6.43	14.10	12.50		
Ho	2.93	4.39	1.46	3.03	2.68		
Er	8.52	12.20	4.25	8.21	7.26		
Tm	1.25	1.74	0.64	1.20	1.00		
Yb	8.31	10.70	4.24	7.54	6.41		
Lu	1.23	1.42	0.63	1.12	0.90		
ΣREE	475.00	388.00	189.00	476.00	407.00		
LREE/HREE	8.76	4.72	6.90	8.35	8.04		
$(La/Yb)_N$	9.09	4.79	5.63	9.66	9.71		
δEu	0.17	0.23	0.37	0.19	0.38		
δCe	0.98	0.90	1.18	0.90	0.90		

*After Wu et al., 2007, the number in bracket is the number of samples. Others from this paper.

mineralization in southern "Sanjiang" area. In this paper, petrological geochemistry and LA-ICP-MS zircon U-Pb isotopic dating results are presented to discuss the age and origin of the Muchang alkali granite and the relationship between the granite and the tectonic-skarn-controlled Pb-Zn deposit.

2 Geological Setting

Western Yunnan in southwest China is composed of several continental blocks. The Baoshan-Zhenkang block, one of the geological bodies in this area, is bordered by NE -trending Lancangjiang and Kejie-Nandinghe faults to the

east and NW-trending Nujiang-Longlin-Luxi fault to the west. There is continuous sedimentation from Paleozoic to Mesozoic with Carboniferous and Triassic volcanic rocks widespread in this region. The study area is located at the south-eastern Fengwei town in south part of the Baoshan-Zhenkang block, and in the junction belt among Gangdese-Nianqingtanggula fold systems, Changning-Menglian fold systems and Fugong-Zhangkang fold systems (Fig. 1). The regional structure is characterized by well-developed NE-trending faults and wide and gentle folds, in which the Nandinghe fault and Zhangkang anticlinorum (NNE-trending axis) are the main fault and fold. The Zhangkang anticlinorum, extending from the Fengwei town in the west to Dashan fault in the southern Kejie Fault in the east and to Nandinghe fault in the south, covers an area of over 1,001,000 km^2. The interior of the Zhenkang anticlinorum is located near Luziyuan-Mangbin and its stratum consist of Upper Cambrian Shahechang Formation ($\epsilon_3 s$: marble intercalated by slate and chloritization quartz schist), which host the Luziyuan Pb-Zn polymetallic deposit, and the Baoshan Formation ($\epsilon_3 b$: clastic and carbonate rocks). From the interior to the edge of anticlinorum, these formations of anticlinal flanks are as follows: Cambrian, Ordovician, Silurian, Devonian, Carboniferous, Permian and Triassic. Minor magmatic activity occurs in this region. With the exceptions of some late Carboniferous basic-intermediate to basic extrusive rocks and late Triassic basic -intermediate to acid extrusive rocks exposed at the flanks of anticlinorum, the Muchang alkali granitic pluton is the main magmatic body. In addition, geological and geophysical studies suggested that unexposed intermediate-acid intrusive rocks in the interior of anticlinorum near the Luziyuan area are related to Pb-Zn-Cu mineralization in the ore district (Zhao et al., 2002; Dong, 2007).

The Muchang alkali granites, which are hosted in the eastern interior of the Zhankang anticline composed of Paleozoic strata and intruded Lower Permian marine sedimentary rocks (Yongde Formation and Shazipo Foremation), Upper Permian alkali basalt ($P_2\beta$) and Middle Triassic Hewanjie Formation(T_2h) limestone, are locate about 20 km to southeast of the Fengwei town. It occurs in groups with small outcrop and irregular shape. The Muchang granitic pluton is the largest one with an area of 4.5 km^2 and has an intrusive contact with Lower Permian Shazipo Formation (P_1s) limestone and dolomitic limestone to the west and with Upper Permian alkali basalt ($P_1\beta$) to the east (Fig. 1). Field investigations revealed that the Muchang granitic pluton is a two-stage intrusion exhibiting rift-related characteristics. The early-stage riebeckite nordmarkite distributes in the east and west sides of the pluton and in the discontinuous marginal zone, and the main body consists of the late-stage dominant riebeckite granite with minor aegirine granite (Fig. 1) (after Gu et al., 1988). All the studied samples are collected from the late-stage riebeckite granitic intrusion. These rocks are grey in color and medium-grained texture with minor fine– to medium-grained texture (granularity: 0.2–0.8 cm, mainly 0.3–0.6 cm). They are composed of K-fieldspars (30%–40%), plagioclase (15%–20%), quartz (30%–40%) with minor muscovite and biotite. The accessory minerals consist of magnetite, ilmenite, apatite, mengite, zircon and pyrite. Weak alteration and local polymetallic Sn mineralization occur near the contact zone. Quartz vein type and structural-altered rock type gold deposit (e.g., Xiaogangou gold deposit) occur in altered basalt from the external contact zone.

3 Analytical Techniques

Major and trace elements analyses were conducted for riebeckite granite from the Muchang pluton. Weathered surfaces of these rocks were removed, cleaned with deionized water, crushed and then powdered with an agate mill. Major oxides were analyzed using a PANalytical Axios-advance X-ray fluorescence spectrometer (XRF) at the State Key Laboratory of Ore Deposit Geochemistry, Institute of Geochemistry, Chinese Academy of Science (SKLODG, IGCAS). Fused glass disc method was used and the analytical precision, as determined on the Chinese National standard GSR-1, was better than 5% (Table 1). Loss on ignition (LOI) was obtained using 1 g of powder heated to 1100°C for 1 h. Trace elements were analyzed using a Plasma Optical Emission Mass Spectrometer (POEMS) ICP-MS system at the SKLODG. The detailed analytical procedures were described by Qi et al. (2000). The precision is better than 5% for all elements on the international standards (GBPG-1 and OU-6), in good agreement with the recommended values (Table 1).

Zircons were separated from six samples (MC08-01, MC08-02, MC08-03, MC08-04, MC08-05 and MC08-06) collected from different sampling locations within the batholith (Fig. 1), using conventional heavy liquid and magnetic techniques. Representative zircon grains were handpicked under a binocular microscope, mounted in epoxy resin, and then polished and coated with gold. Zircons were documented with transmission and reflecting light microscopy as well as under cathodoluminescence (CL) images to reveal their internal structures. U-Pb isotopic analyses for zircons were conducted using an Elan 6100 DRC ICP-MS equipped with 193 nm Excimer lasers at the State Key Laboratory of Continental Dynamics, Department of Geology, Northwest University, Xi'an, China. Zircon 91500 was used as a standard and NIST 610

was used to optimize the machine. A mean age of 1062 Ma was obtained for the 91500 zircon standard. The spot diameter was 30 μm. Corrections for common-Pb were made using the method of Andersen (2002). Data were processed using the GLITTER and ISOPLOT (Ludwig, 2003) programs. Errors on individual analyses by LA-ICP-MS are quoted at the 95% (1r) confidence level. The details of the analytical procedures have been described by Yuan et al. (2004) and Qin et al. (2008).

4 Major and Trace Elements

4.1 Major elements

The analytical results for whole rocks (Table 1) show that the Muchang alkali granite are characterized by the following characteristics: (1) enrichment in SiO_2, the $\omega_{(SiO_2)}$ is abnormally high (averaging 74.90 wt%, n=5) with a narrow range between 71.57 wt% and 76.66 wt%, quite different from that of the Lincang and Pinghejie S-type granites ($\omega_{(SiO_2)}$=67.00 wt%–70.00 wt%) in this region (Liu et al., 1989), and similar to A-type granites in China and worldwide (Wu et al., 2007); (2) Enrichment in Al_2O_3, the $\omega_{(Al_2O_3)}$ range from 13.00 wt% to 15.48 wt% with an average of 13.88 wt% (n=5). The A/CNK ratios (1.30–1.57, averaging 1.47) are higher than 1.00. In the A/CNK-A/NK diagram, all samples are plotted in the peraluminous field (omitted), indicating that these rocks belong to aluminum oversaturated series rocks; (3) enrichment in alkaline, the $\omega_{(K_2O)}$, $\omega_{(Na_2O)}$, and $\omega_{(K_2O+Na_2O)}$ range between 4.43 wt% and 5.32 wt% (averaging 4.82 wt%), 1.93 wt% and 3.15 wt% (averaging 2.39 wt%) and 6.50 wt% and 8.47 wt% (averaging 7.21 wt%) with K_2O/Na_2O ratios higher than 1.00 (1.69–2.50, averaging 2.06), respectively; (4) depletion in CaO and MgO, the CaO contents vary from trace to 0.55 wt% with an average of 0.22 wt%, and MgO contents range from 0.02 wt% to 0.58 wt% with an average of 0.23 wt%; (5) depletion in Ti and P, the $\omega_{(TiO2)}$ is between 0.25 wt% and 0.57 wt% (averaging 0.38 wt%), the $\omega_{(P2O5)}$ are mostly lower than 0.01 wt%, different from that of Al-rich S-type granite (generally > 0.10 wt%); (6) high FeO_T/MgO ratio, they range from 4.66 to 155 with an average of 56.59, much higher than those of I-type and S-type granites (Whalen et al., 1987), and similar to that of the global average value of A-type granites (Turner et al., 1992). In the Q-A-P diagram, all the Muchang samples are plotted in the field of alkali granites (Fig. 2). Normally, for high silica type granite (SiO_2>74.00 wt%), the diagram of (FeO_T/MgO)-SiO_2 is the most effective to distinguish the A-type granite from I-type and S-type granite (Eby, 1990). With the exception of one sample, the samples of Muchang are plotted in the field of A-type granites in the diagram (Fig. 3), distributed in the same field with Australian Mumbulla

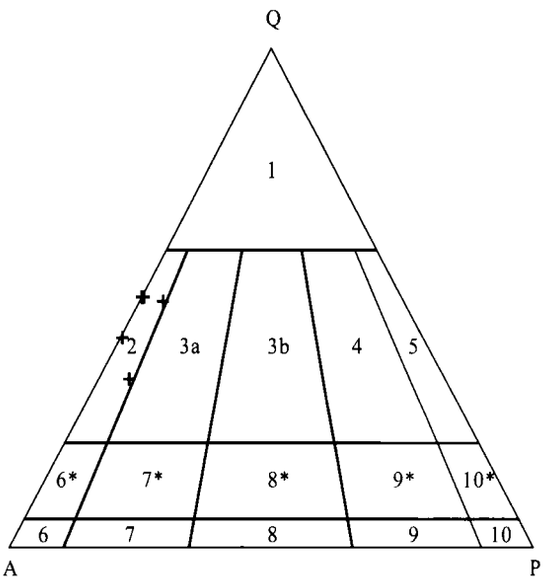

Fig. 2. Q-A-P diagram for the Muchang alkali granites.

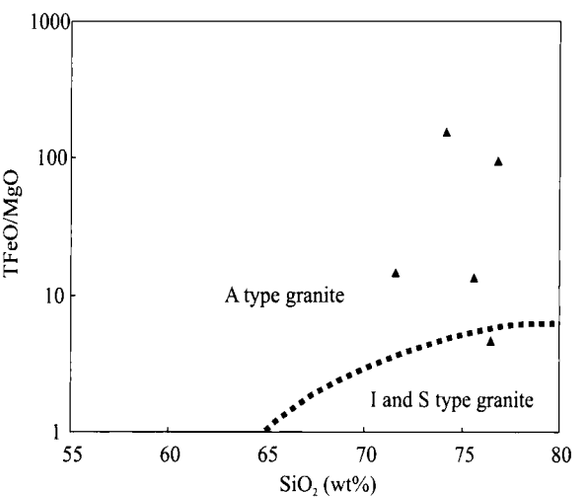

Fig. 3. FeO_T-SiO_2 diseriminant diagram for the Muchang alkali granites (After Eby, 1990).

A-type granite (Whalen et al., 1987) and the aluminous A-type granites in the coastal area of Fujian Province , China (Qiu et al., 2000). In summary, the characteristics of the Muchang granite are similar to those of A-type granites worldwide and quite different from those of I-type and S-type granite in the world (King et al., 1997; Wu et al., 2007).

4.2 Rare and trace elements

Table 1 shows that the total REE contents of the Muchang granites are similar to those of A-type granites and two times higher than that of normal granites, ranging from 189.26 ppm to 475.61 ppm (mostly >350.00 ppm) with an average of 386.89 ppm (n=5). The chondrite-normalized REE distribution patterns of the granites exhibit enrichment in light REE (LREE) with high LREE/HREE ratios (4.72–8.76), and $(La/Yb)_N$ ratios (4.79–9.71), variable $(La/Sm)_N$ ratios (2.95–5.42). Their low $(Gd/Yb)_N$ ratios (1.00–1.50) indicate a weak HREE fractionation. All

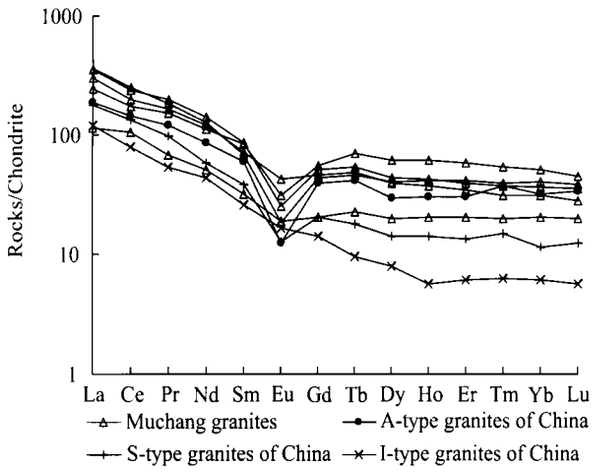

Fig. 4. Chondrite-normalized REE patterns of the Muchang alkali granite (Chondrite values after Sun and McDonough, 1989); A-type, S-type and I-type granite of China after Wu et al., 2007).

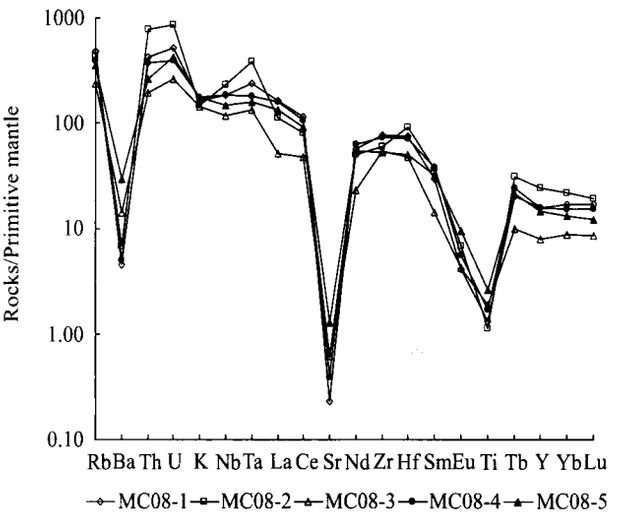

Fig. 5. Spider diagram of traced elements for the Muchang alkali granite (Primitive mantle values after Sun and McDonough, 1989).

samples display strongly negative Eu-anomalies (δEu=0.17 –0.38) (Table 1, Fig. 4) with weak Ce anomaly (δCe=0.90–1.18). REE distribution patterns of the Muchang granites exhibit enrichment in LREE, typical of A-type granite (Fig. 4). The REE compositions of the Muchang granites are comparable to those of A-type granites in China and different from that of I-type and S-type granites in China.

The Muchang granites are characterized by high abundances of Rb (149.00 ppm–305.00 ppm, averaging 241.20 ppm) and Nb (83.90 ppm–165.00 ppm, averaging 123.58 ppm) , and its concentrations are higher than that of A-type granite (Whalen et al., 1987). They are significantly enriched in lithophile elements (e.g., Rb, K, U, and Th) and high field strength elements (e.g., Zr, Hf, Nb, Y, Ga) and depleted in Sr, Ba, Ti, Cr and Ni (Table 1). In the primitive mantle-normalized spidergram, the Muchang granites show significant depletion in Ba, Sr and Ti (Table 1, Fig. 5) but no Nb and Ta anomalies, similar to aluminous A-type granite and different from S-type granites (Qiu et al., 2000). Furthermore, Rb/Sr and Rb/Ba ratios of these rocks range from 8.50 to 62.5 (averaging 26.8) and 1.11 to 9.65 (averaging 5.02), respectively, much higher than those of A -type granites worldwide (Rb/Sr=3.52, Rb/Ba=0.48, Whalen et al., 1987) and similar to those of A-type granites in China (Rb/Sr=20.6 and Rb/Ba=8.94, Wu et al., 2007). These characteristics imply that these rocks experienced high degree of magma evolution. Ga/Al ratios of the Muchang granites vary from 3.52 to 4.19 with an average of 3.84, obviously higher than the average values of S-type and I-type granites (2.3 and 2.1, Whalen et al., 1987). In the diagrams of $(Na_2O+K_2O)/CaO$, K_2O/MgO, Ce, Nb, Y, Zn, Zr and AKI value vs. 10000×Ga/Al (Fig. 6) and SiO_2-Zr

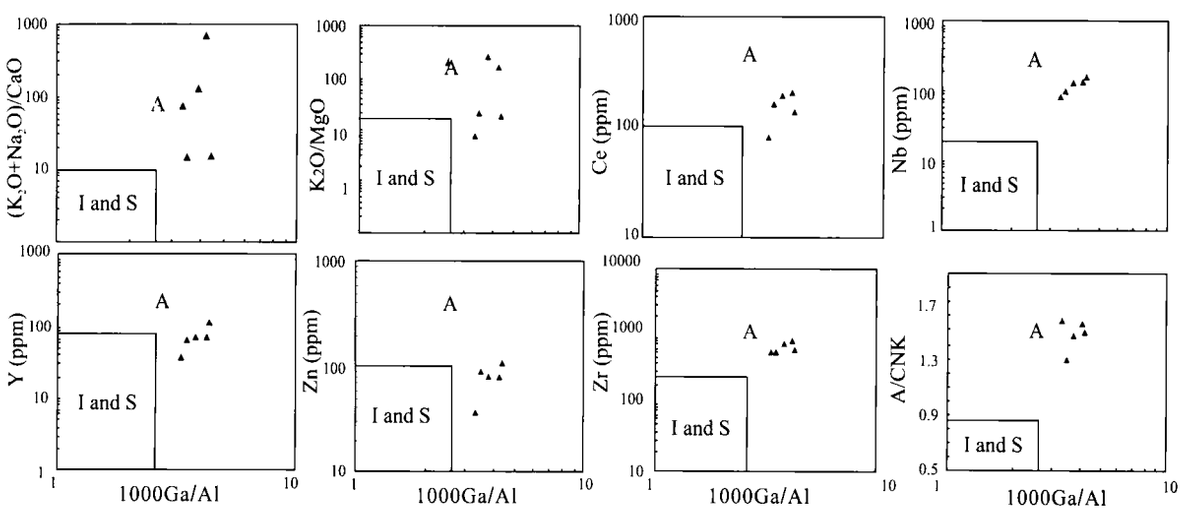

Fig. 6. $(Na_2O+K_2O)/CaO$, K_2O/MgO, Ce, Nb, Y, Zn, Zr and AKI vs. 10000×Ga/Al plots of aluminous A-type granites from the Muchang.
I, S and A is I-type, S-type and A-type granite respectively.

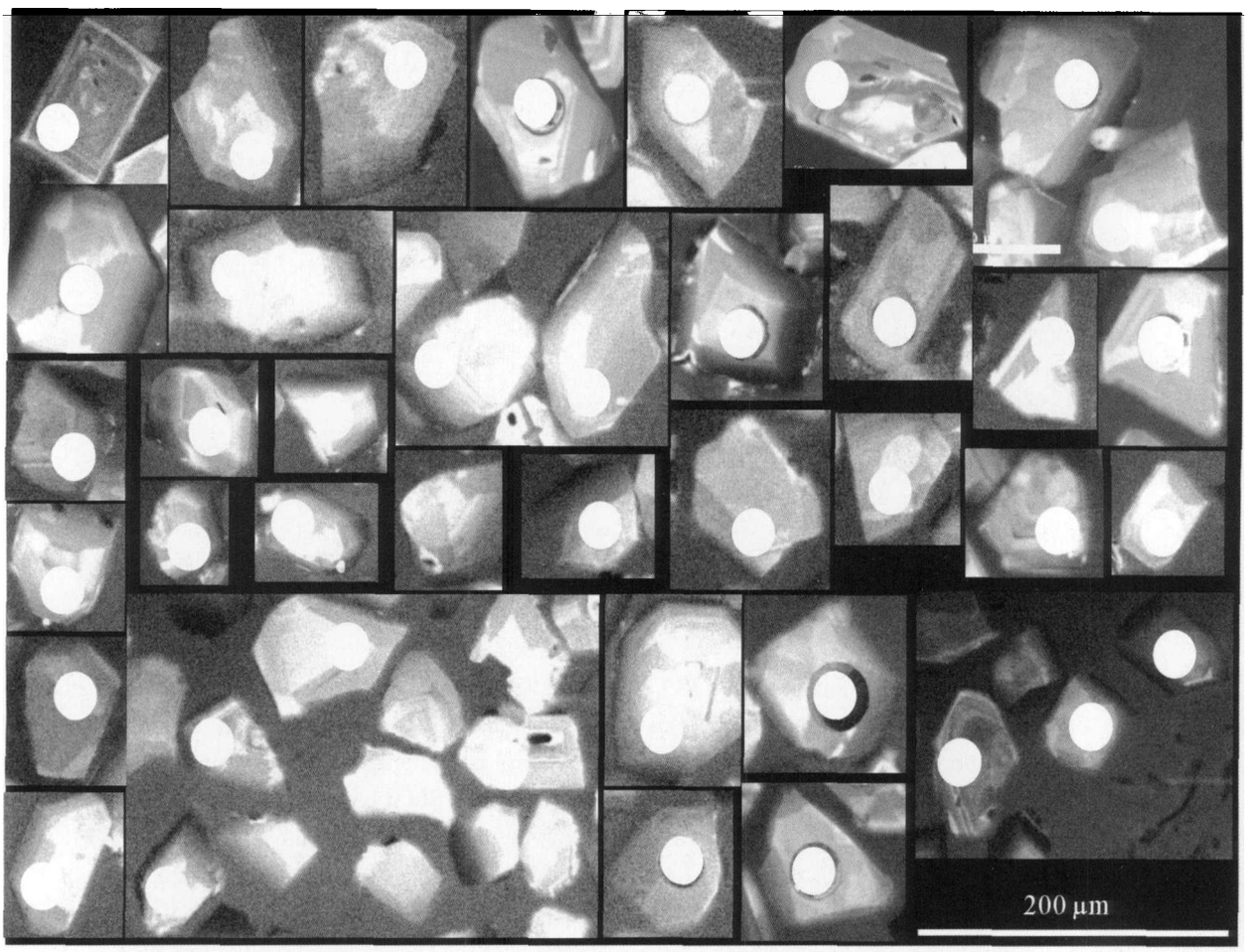

Fig. 7. Cathodoluminescence images of zircons from the Muchang alkali granites and spot sites.

and SiO_2-Nb (omitted), all the studied Muchang granites are plotted in the field of A-type granites, indicating that trace elements contents of these rocks are similar to aluminous A-type granites (Whalen et al., 1987; King et al., 1997; Qiu et al., 2000). Their Zr+Nb+Ce+Y contents vary from 799.00 ppm to 1253.00 ppm with an average of 1052.00 ppm, much higher than the lowest of A-type granite (350.00 ppm, Whalen et al., 1987). All samples are plotted in the field of A-type granites in the Ga/Al vs. (Zr+Nb+Ce+Y) (omitted). As shown above, it is suggested that the Muchang granites belong to A-type granites.

5 Zircon U-Pb Age

Abundant zircons in the studied granite samples are euhedral, long columnar or semi-conoid, up to 100 μm in size. Most of them are transparent to light brown in color, and exhibit magmatic oscillatory zoning in the cathodoluminescence images (Fig. 7), showing that they belong to magma crystallized zircons (Wu and Zheng, 2004). Forty-five spots of forty grains from the Muchang samples were analyzed, of which thirty spots gave good results, the others were breakdown by laser beam and excluded for calculating the age (Table 2). The analytical results show that U and Th contents range from 119.00 ppm to 1025.00 ppm and 58.20 ppm to 569.00 ppm respectively, and their corresponding Th/U ratios (0.31–0.80, averaging 0.51) are higher than 0.10, implying that these zircons belong to magmatic origin (Rubatto and Gebauer, 2000; Belousova et al., 2002; Moller et al., 2003). LA-ICP-MS data on 30 grains from the Muchang sample yielded a weighted mean age of 266.2±5.4 Ma (2σ) (Table 2, Fig. 8). In summary, U-Pb data indicate that the Muchang granite crystallized at ca. 266 Ma.

6 Discussion

6.1 Petrogenetic type

All the studied granite samples belong to high-aluminum (Al_2O_3: 13.00 wt%–15.48 wt%) series, displaying high SiO_2 (71.57 wt%–76.66 wt%), FeO_T/MgO ratio (4.66–155) and Na_2O+K_2O (>4.4%, K_2O/Na_2O higher than 1.00), and low CaO (trace–0.55 wt%) and MgO (0.02 wt%–0.58 wt%), similar to those of A-type granites (Collins et al., 1982; Whalen et al., 1987). REE distribution patterns of the Muchang granites (LREE enrichment) also resemble that of typical A-type granite. They are obviously enriched in lithophile elements (e.g., Rb, K, U, Th) and high field

Table 2 The LA-ICPMS U-Pb dating of Muchang granite

Sample	U (ppm)	Th (ppm)	Pb (ppm)	$^{238}U/^{232}Th$	Isotopic ratios						Age (Ma)					
					$^{207}Pb/^{206}Pb$	1σ	$^{207}Pb/^{235}U$	1σ	$^{206}Pb/^{238}U$	1σ	$^{207}Pb/^{206}Pb$	1σ	$^{207}Pb/^{235}U$	1σ	$^{206}Pb/^{238}U$	1σ
MC-15-1	141	82.6	6.13	1.72	0.1	61.92	0.27192	0.00858	0.04303	0.00061	0.1	61.92	244.2	6.85	271.6	3.76
MC-15-2	166	95.3	7.39	1.75	399.1	57.19	0.32846	0.00871	0.04356	0.00060	399.1	57.19	288.4	6.65	274.9	3.73
MC-15-3	202	119.0	13.15	1.69	409.8	61.72	0.31850	0.00913	0.04204	0.00059	409.8	61.72	280.8	7.03	265.4	3.67
MC-15-4	169	92.9	7.28	1.82	163.0	59.12	0.28519	0.00747	0.04193	0.00058	163.0	59.12	254.8	5.90	264.8	3.56
MC-15-5	148	81.8	6.52	1.82	344.1	59.93	0.31061	0.00847	0.04221	0.00059	344.1	59.93	274.7	6.56	266.5	3.63
MC-15-6	137	58.2	6.04	2.38	180.3	67.19	0.30842	0.00915	0.04501	0.00063	180.3	67.19	273.0	7.10	283.8	3.90
MC-15-7	152.	98.7	6.75	1.54	261.8	61.82	0.29628	0.00822	0.04174	0.00058	261.8	61.82	263.5	6.44	263.6	3.60
MC-15-8	478	201.0	21.81	2.38	91.7	49.94	0.29997	0.00651	0.04544	0.00060	91.7	49.94	266.4	5.08	286.5	3.73
MC-15-9	149	79.2	6.74	1.89	319.3	58.55	0.31863	0.00849	0.04377	0.00060	319.3	58.55	280.8	6.54	276.2	3.73
MC-15-10	119	95.4	6.32	1.25	396.8	162.78	0.34275	0.02583	0.04550	0.00090	396.8	162.78	299.3	19.54	286.8	5.53
MC-15-11	152	71.2	6.57	2.13	377.8	70.82	0.31441	0.01014	0.04209	0.00061	377.8	70.82	277.6	7.83	265.7	3.78
MC-15-12	142	77.8	6.10	1.82	137.4	71.53	0.27984	0.00874	0.04159	0.00059	137.4	71.53	250.5	6.93	262.7	3.67
MC-15-13	158	100.0	6.75	1.56	401.5	61.92	0.31740	0.00911	0.04204	0.00059	401.5	61.92	279.9	7.02	265.5	3.67
MC-15-14	356	120.0	14.10	2.94	117.6	53.19	0.26836	0.00630	0.04022	0.00054	117.6	53.19	241.4	5.04	254.2	3.36
MC-15-15	191	88.9	8.08	2.13	104.7	60.11	0.28323	0.00744	0.04269	0.00059	104.7	60.11	253.2	5.89	269.5	3.62
MC-15-16	181	91.4	7.57	2.00	178.0	66.70	0.27337	0.00803	0.03993	0.00056	178.0	66.70	245.4	6.40	252.4	3.49
MC-15-17	307	112.0	12.92	2.78	423.4	52.07	0.31721	0.00773	0.04161	0.00057	423.4	52.07	279.8	5.96	262.8	3.51
MC-15-18	143	82.2	6.59	1.75	140.1	64.94	0.29426	0.00836	0.04369	0.00061	140.1	64.94	261.9	6.56	275.6	3.77
MC-15-19	243	139.0	10.39	1.75	350.8	57.87	0.29968	0.00789	0.04060	0.00056	350.8	57.87	266.2	6.16	256.5	3.48
MC-15-20	297	119.0	12.00	2.50	223.6	59.26	0.28224	0.00745	0.04043	0.00056	223.6	59.26	252.4	5.90	255.5	3.46
MC-15-21	186	65.3	7.65	2.86	201.3	66.27	0.28097	0.00821	0.04064	0.00057	201.3	66.27	251.4	6.51	256.8	3.56
MC-15-22	157	102.0	8.54	1.54	419.7	71.84	0.30869	0.01017	0.04056	0.00060	419.7	71.84	273.2	7.89	256.3	3.69
MC-15-23	271	139.0	11.37	1.96	285.9	60.97	0.29154	0.00797	0.04065	0.00057	285.9	60.97	259.8	6.27	256.8	3.52
MC-15-24	161	75.8	6.89	2.13	390.0	66.74	0.30939	0.00942	0.04120	0.00059	390.0	66.74	273.7	7.31	260.2	3.67
MC-15-25	126	71.7	5.42	1.75	392.2	76.80	0.30577	0.01074	0.04068	0.00061	392.2	76.80	270.9	8.35	257.0	3.77
MC-15-26	188	92.2	8.12	2.04	117.6	72.60	0.27967	0.00878	0.04193	0.00060	117.6	72.60	250.4	6.97	264.8	3.74
MC-15-27	137	69.6	5.92	1.96	135.4	83.81	0.27985	0.01016	0.04164	0.00062	135.4	83.81	250.5	8.06	263.0	3.86
MC-15-28	152	74.0	6.42	2.04	202.9	80.72	0.28001	0.00990	0.04047	0.00060	202.9	80.72	250.7	7.86	255.8	3.74
MC-15-29	266	82.3	10.83	3.23	223.2	68.09	0.28717	0.00861	0.04115	0.00059	223.2	68.09	256.3	6.79	259.9	3.65
MC-15-30	1025	569.0	47.20	1.79	199.3	58.82	0.30224	0.00782	0.04376	0.00061	199.3	58.82	268.1	6.10	276.1	3.76

Th and U contents are given directly, Pb = $^{204}Pb\times0.014 + ^{206}Pb\times0.241 + ^{207}Pb\times0.221 + ^{208}Pb\times0.524$.

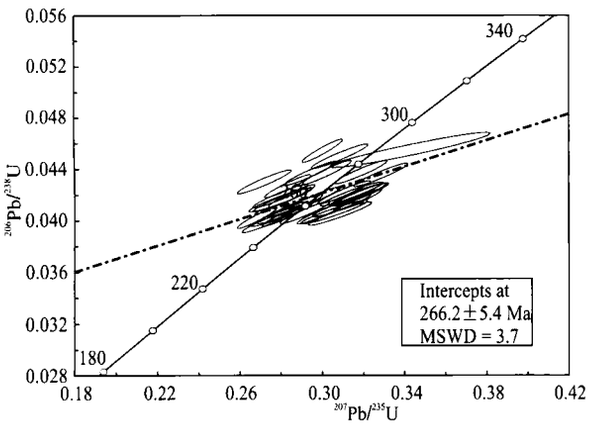

Fig. 8. Concordia diagram of zircon LA-ICP-MS U-Pb age of the Muchang alkali granites.

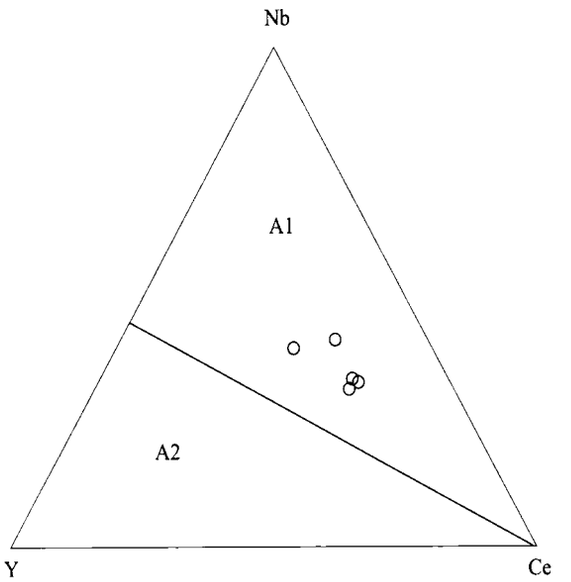

Fig. 9. Diagram of Nb-Y-Ce of A-type granite (after Eby, 1990).

A1, non-collision A-type granite; A2, post-collision A-type granite.

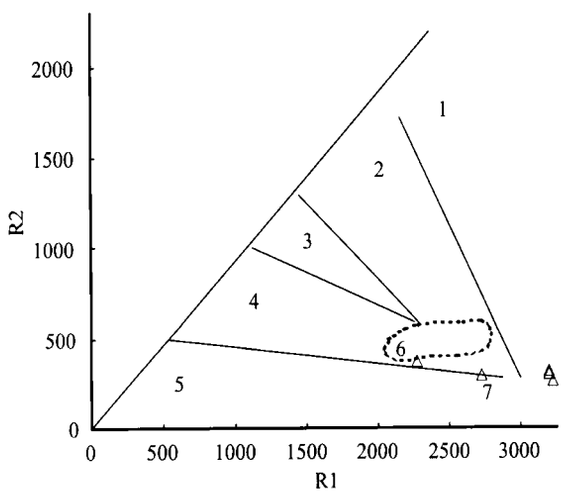

Fig.10. R1 vs R2 plot of major elements for tectonic discrimination (after Batchelor and Bowden, 1985).

1, product of mantle differentiation; 2, pre-plate collision; 3, uplift of post collision; 4, late orogenic stage; 5, non-collision; 6, syn-collosion; 7, post-collision.

strength elements (e.g., Zr, Hf, Nb, Y, Ga) with high 10000×Ga/Al ratios (3.52–4.19) and Zr+Nb+Ce+Y, and depleted in Sr, Ba, Ti, Cr and Ni. In all diagrams for discriminating tectonic setting of granites, the Muchang granites are plotted in the field of A-type granite, indicating that these rocks share similar feature to aluminous A-type granites (Whalen et al., 1987; King et al., 1997; Qiu et al., 2000; Wu et al., 2007) and quite different from those of I-type and S-type granites worldwide (King et al., 1997; Li et al., 2007; Qin et al., 2008; ; Yang et al., 2008).

6.2 Tectonic significance

Statistical research on the distribution of trace elements for granite which occur in different tectonic setting, the diagram for discriminating tectonic setting of Y–Nb, Yb+Nb–Rb, Yb+Ta–Rb, Ta–Yb and trigonal diagram for discriminating tectonic setting of Rb/10–Hf–3×Ta and Rb/30–Hf–3×Ta are proposed to distinguish granites of different origins (Pearce et al.,1984). In these discriminating diagrams, the projection points of the Muchang granite distribute in the within-plate granites region (omitted). Generally, the granites formed in compression environment process have lower Gd/Lu ratios (8–12) and that formed in extensional environment process have Gd/Lu ratios higher than 15 (Whalen et al., 1987). The Gd/Lu ratios of the Muchang granites vary between 21.3 and 37.5, indicating that these rocks were formed in an extensional environment.

The generation of A-type granites is related to the extension tectonics of lithosphere (Loiselle and Wones, 1979). Previous studies show that these A-type rocks can be divided into two groups, one is non-collision type, named by A1 (or AA) type, and another is post-collision type, named by A2 (or PA) type (Whalen et al, 1987; Eby, 1992). Both of them have different material sources and formed in different tectonic setting, in which, A1 (or AA) type granites came from oceanic island arc basalt, and intruded in continental rift or intruded during within-plate magmatic process. Its tectonic setting belongs to the extension after the stability of continental lithosphere and is the signature of the beginning of rift activity; A2 (or PA) type granites came from the continental crust or low crust under plated which went through the continent-continent collision or arc magmatism. It is the signature of the extension of end of orogeny. In these discriminating diagrams of Nb-Y-Ce (Fig. 9), Nb-Y-3Ga (omitted) and R1-Ga/Al (omitted), the Muchang samples are plotted in the field of A1 (or PA). These rocks show the character of the post orogenic granite in the diagram of R1-R2 (Fig. 10), indicating that the Muchang granites were formed during the extensional stage at the end of post-collision.

6.3 Age of the Muchang granite and its implication

As one of an the important parts of east Tethys tectonic belt, numerous geological and geochemical studies focus on the relationship between geological tectonic setting and evolution of Tethys tectonic belt in western Yunnan Province, China (Zhong et al., 1998; Wang, 1996; Zhang et al., 1997; Pan et al., 2003; Wang et al., 2009; Deng et al., 2010). Due to the lack of systematic and precise isotopic dating results in this region, different researchers have different explanations for the age of continent-continent collision or continent-arc collision during the evolution of Proto-Tethys induced from studies on the giant S-type Linchang granitic batholith (e.g. Lincang, Pinghejie, e.g. 279–210 Ma (Chen, 1989), 292–275 Ma (Liu et al.,1989), 255–180 Ma (Qin, 1991), 288–138 Ma (Mo et al.,1998), 230–229 Ma (Peng et al., 2006), 250–246 Ma (Liu et al., 2008). The Muchang A-type granite belongs to A1 (or AA) type, showing the signature of the beginning of rift activity. LA-ICP-MS zircon U-Pb data of the Muchang granites gave a weighted mean age of 266.2±5.4 Ma, indicating the tectonic setting of this region is in the extensional stage at the end of post-collision at Middle Permian and implying the consumption of Paleo-Tethys Ocean took place before 266 Ma. Different isotopic age of giant S-type Linchang granites batholith may show continent-continent collision or Continent-arc collision continue a long history from Early Permian to Early Triassic.

6.4 Relationship between the Luziyuan Pb-Zn deposit and the Muchang granites

The Luziyuan Pb-Zn deposit is located in the NNW-direction, 14 km from the Muchang granites, near the EN-trending fault and interlayer fracture zone at the core of the Zhenkang anticline. The stratified and vein-type Pb-Zn-polymetallic orebodies hosted in skarn and marbleized limestone of the Upper Cambrian Shahechang Formation ($\epsilon_3 s$: marble intercalated by slate and chloritization quartz schist). The deposit consists of three sectors with a total reserve of over 1.9 million tons of Pb+Zn, 0.12 million tons of Cu and 500 tons of Ag. On the basis of geophysical investigation, it is suggested that there are unexposed intermediate-acid intrusive rocks in the ore district, which is the "sister" rocks material of the Muchang granites and related to Pb-Zn mineralization (Zhao et al., 2002; Dong, 2007). The present study shows that the Muchang granites were formed at Early Indochina epoch, implying the unexposed intermediate-acid intrusive rocks are the product of Middle Permian, associated with different types of mineralization (e.g., Pb, Zn, Cu and Sn) in this region, such as the Luziyuan Pb-Zn deposit, Wumulan Sn deposit (Dong, 2007) etc.

7 Conclusions

On the basis of the above discussion, it is concluded that:

(1)The Muchang alkali granites belong to A-type granites, characterized by high Al_2O_3, SiO_2 and FeO_T/MgO ratio with low CaO and MgO. REE distribution patterns of the Muchang granites exhibit LREE enrichment, and special seagull-type in shape, similar to that of typical A-type granite. They are obviously enriched in lithophile elements (e.g., Rb, K, U, and Th) and high field strength elements (e.g., Zr, Hf, Nb, Y, Ga) with high 10000×Ga/Al ratios and depleted in Sr, Ba, Ti, Cr and Ni.

(2)LA-ICP-MS zircon U-Pb data of the Muchang granites yielded a weighted mean age of 266.2±5.4 Ma (2σ), showing that they were formed at Middle Permian.

(3)These rocks were formed in the extensional stage at the end of post-collision at Middle Permian, implying that the consumption of Paleo-Tethys Ocean took place before 266 Ma.

Acknowledgements

This research project was jointly supported by the National "973 Project" (No. 2009CB421003), the Knowledge Innovation Program of the Chinese Academy of Sciences (Grant No: KZCX2-YW-136-2, KZCX2-YW-111-03), and the Foundation of State Key Lab. Of Ore Deposit Geochemistry. We are greatly indebted to Professor Zhong Hong who carefully read through the entire paper and made many constructive suggestions. The authors are grateful to the State Key Laboratory of Continental Dynamics, Department of Geology, Northwest University for U-Pb zircon LA-ICP-MS dating.

Manuscript received July 9, 2010
accepted August 24, 2010
edited by Liu Xinzhu and Liu Lian

References

Andersen, T., 2002. Correction of common lead in U-Pb analyses that do not report ^{204}Pb. *Chemical Geology*, 192: 59–79.

Batchelor, R.A., and Bowden, P., 1985. Petrogenetic interpretation of granitoid rock series using multicationic parameters. *Chemical Geology*, 48: 43–55.

Belousova, E.A., Griffin, W.L., and Reilly, S.Y., 2002. Igneous zircon: Trace element composition as an indicator of source rock type. *Contributions to Mineralogy and Petrology*, 143(2): 602–622.

Black, R., and Liegeois, J.P., 1993. Cratons, mobile belts, alkaline rocks and continental lithospheric mantle; the Pan-African testimony. *J. Geol. Soc.* (Lond.), 150: 89–98.

Bonin, B., 2007. A-type granites and related roeks: Evolution of a concept, problems and prospects. *Lithos*, 97: 1–29.

Chen Jicheng, 1987.The discussion of chronological division of granites and selection of isotopic ages. *Yunnan Geology*, 6: 101–113 (in Chinese).

Chen Yongqing, Lu Yingxiang, Xia Qinlin, Jiang Chengxing, Liu Hongguang and Lu Zhicheng, 2005. Geochemical characteristics of the Hetaoping Pb-Zn deposit, Baoshan, Yunnan, and its genetic model and ore prospecting model pattern. *Geology in China*, 32(1): 90–99 (in Chinese with English abstract).

Collins, W.J., Beams, S.D., White, A.J.R., and Chappell, B.W., 1982. Nature and origin A-type granites with particular reference to Southeastern Australia. *Contributions to Mineralogy and Petrology*, 80: 189–200.

Deng Bifang, 1995. Metallogenic model of mercury and lead-zinc deposits in Baoshan-Zhenkang area. *Yunnan Geology*, 14 (4): 355–364 (in Chinese).

Deng Jun, Hou Zengqian, Mo Xuanxue, Yang Liqiang, Wang Qinfei and Wang Changming, 2010. Superimposed orogenesis and metallogenesis in Sanjiang Tethys. *Mineral Deposits*, 29 (1): 37–42 (in Chinese with English abstract).

Dong Wenwei, 2007. The metallogenetic conditions and typical model in Baoshan-Zhenkang massif. *Yunnan Geology*, 26(1): 56–61 (in Chinese with English abstract).

Dong Wenwei and Chen Shaolin, 2007. The characteristics and genesis of Luziyuan Pb-Zn deposit, Zhenkang. *Yunnan Geology*, 26(4): 404–410 (in Chinese with English abstract).

Eby, G.N., 1990. The A-type granitiods: A review of their occurrence and chemical characteristics and speculations on their petrogenesis. *Lithos*, 26: 115–134.

Eby, G.N., 1992. Chemical subdivision of the A-type granitoids; petrogenetic and tectonic implications. *Geology*, 20: 641–644.

Fan Weiming, Peng Touping and Wang Yuejun, 2009. Triassic magmatism in the southern Lancangjiang zone, southwestern China and its constraints on the tectonic evolution of Paleo-Tethys. *Earth Science Frontiers*, 16(6): 291–302 (in Chinese with English abstract).

Gu Yingqu, Qian Tianhong, Ye Zhishan and Yan Yibin, 1988. The Petrographic and Geochemical Characteristics of the Muchang A-type Granite in Zhenkang, Western Yunnan. *Acta Petrological et Mineralogical*, 7(1): 38–48 (in Chinese with English abstract).

He Chuansong, Zhu Lupei and Wang Qingcai, 2009. The Significance of Crust Structure and Continental Dynamics inferred from Receiver Functions in West Yunnan. *Acta Geologica Sinica* (English edition), 83(6): 1163–1172.

King, P.L., White, A.J.R., Chappell, B.W., and Allen, C.M., 1997. Characterization and origin of aluminous A-type granites from the Lachlan Fold Belt, southeastern Australia. *J. Petrol.*, 38: 371–391.

Li, X.H., Li, Z.X., Li, W.X., Liu, Y., Yuan, C., Wei, G.J., and Qi, C.S., 2007. U-Pb zircon, geochemical and Sr-Nd-Hf isotopic constraints on age and origin of Jurassic Iand A-type granites from central Guangdong, SE China: a major igneous event in response to foundering of a subducted flat-slab? *Lithos*, 96: 186–204.

Litvinovsky, B.A., Jahn, B. M., Zanvilevich, A.N., Saunders, A., Poulain, S., Kuzmin, D.V., Reichow, M.K., and Titov, A.V., 2002. Petrogenesis of syenite-granite suites from the Bryansky Complex (Transbaikalia, Russia): implications for the origin of A-type granitoid magmas. *Chem. Geol.*, 189: 105–133.

Liu Changshi, Zhu Jinchu, Xu Xisheng, Chu Xuejun, Cai Dekun and Yang Ping, 1989. Study on the characteristics of Lincang composite granite batholith in West Yunnan. *Geology in Yunnan*, 8(3 – 4): 189–204 (in Chinese with English abstract).

Liu Deli, Liu Jishun, Zhang Caihua and Zhou Yuguo, 2008. Geological characteristics and tectonic setting of Yunxian gran ite in the northern part of South Lancangj iang convergent margin, Western Yunnan Province. *Acta Petrological et Mineralogical*, 27(1): 23–31 (in Chinese with English abstract).

Loiselle, M.C., and Wones, D.R., 1979. Characteristics and origin of anorogenic granites. *Geological Society of America Abstracts with programs*, 11: 468.

Ludwig, K.R., 2003. *ISOPLOT 3.0: a geochronological toolkit for Microsoft excel*, Berkeley Geochronology Center. Special publication no. 4.

Martin, R.F., 2006. A-type granites of crustal origin ultimately result from open-system fenitizalion-type reactions in an extensional environment. *Lithos*, 91:125–136

Mingram, B., Trumbull, R.B., Littman, S., and Gerstenberger, H., 2000. A petrogenetic study of anorogenic felsic magmatism in the Cretaceous Paresis ring complex, Namibia: evidence for mixing of crust and mantle-derived components. *Lithos*, 54: 1–22.

Mo Xuanxue, Shen Shengyue and Zhu Qinwen, 1998. *Volcanics-ophiolite and Mineralization of Middle-Southem Part in Sanjiang area of Southwestern China*. Beijing: Geological Publishing House, 1–128 (in Chinese with English abstract).

Moller, A., O'Brien, P.J., and Kennedy, A., 2003. Linking growth episodes of zircon and metamorphic textures to zircon chemistry: An example from the ultrahigh-temperature granulites of Rogaland (SW Norway). *EMU Notes in Mineralogy*, 5: 65–82.

Mushkin, A., Navon, O., Halicz, L., Hartmann, G., and Stein, M. 2003. The petrogenesis of A-type magmas from the Amram Massif, southern Israel. *J. Petrol.*, 44: 815–832.

Pan Guitang, Xu Qiang, Hou Zengqian, Wang Liquan, Du Dexun, Mo Xuanxue, Li Dingmou, Wang Mingjie, Li Xingzheng, Jiang Xingshen and Hu Yunzhong. 2003. *Arckipelagic orogenesis metallogenic systems and assessment of the mineral resources along the Nujiang-Lanchangjiang-Jinshajiang area in southwestern China*. Beijing: Geological Publishing House, 278–420 (in Chinese).

Pearce, J.A., Harris, N.B.W., and Trindle, A.G., 1984. Trace element discrimination diagrams for the tectonic interpretation of granitic rocks. *J. Pertol.*, 25(4): 956–983.

Peng Touping, Wang Yuejun and Fan Weiming, 2006. Zircon SHRIMP U-Pb dating of Early Mesozoic acidity volcanic rock in Southern Laneangjiang and its tectonic significance. *Science in China* (Series D), 36(2): 123–132 (in Chinese).

Qin Jiangfeng, Lai Shaocong, Wang Juan and Li Yongfei, 2008. Zircon LA-ICP MS U-Pb Age, Sr-Nd-Pb isotopic compositions and geochemistry of the Triassic post-collisional Wulong adakitic granodiorite in the south Qinling, central China, and its petrogenesis. *Acta Geologica Sinica* (English edition), 82(2): 425-437.

Qi Liang, Hu Jing and Conrad, G.D., 2000. Determination of trace elements in granites by inductively coupled plasma mass spectrometry. *Talanta*, 51(3): 507–513.

Qin Yuanji, 1999. *The basic characteristics and intrusive mechanism of Lincang granitic batholith*. Beijing: Institute of

Geology, Chinese Academy of Sciences (in Chinese).

Qiu Jiansheng, Wang Dezi and Satoshi Kanisawa, 2000. Geochemistry and petrogenesis of aluminous A-type granites in the coastal area of Fujian Province. *Geochinica*, 29(4): 313–321 (in Chinese with English abstract).

Rubatto, D., and Gebauer, D., 2000. *Use of cathodoluminescence for U-Pb zircon dating by IOM Microprobe: Some examples from the western Alps. Cathodoluminescence in Geoscience*, Springer-Verlag BerlinHeidelberg, Germany, 373–400.

Shellnutt, J.G., and Zhou, M.F., 2007. Permian peralkaline, peraluminous and metaluminous A-type granites in the Panxi distriet, SW China: Their relationship to the Emeishan mantle plume. *Chemieal Geology*, 243: 286–316

Skjerlie, K.P., and Johnston, A.D., 1993. Vapor-absent melting at 10 k bar of a biotite- and amphibole-bearing tonalitic gneiss: implications for the generation of A-type granites. *Geology*, 20: 263–266.

Sun, S.S., and McDonough, W.F., 1989. Chemical and isotopic systematics of oceanic basalts: implication for mantle composition and processes. In: Saunders, A.D. and Norry, M.J. (eds.), *Magmatism in the Oceanic Basins*. Geological Society, London, 42: 313–345.

Turner, S.P., Foden, J.D., and Morrison, R.S., 1992. Derivation of some A-type magmas by fractionation of basaltic magma: an example from the Padthaway Ridge, South Australia. *Lithos*, 28: 151–179.

Wang Anjian, Cao Dianhua, Guan Ye, Liu Junlai and Li Wenchang, 2009. Metallogenic belts of southern three rivers region, Southwest China: distribution, characteristics and Ddiscussion. *Acta Geologica Sinica*, 83(10): 1365–1375 (in Chinese with English abstract).

Wang Kaiyuan, 1996. The pre-Cambrian basement rock group and structural evolution in the SW Sanjiang structural zone and the west margin of Yangzi platform. *Yunnan Geology*, 15 (2): 138–148.

Whalen, J.B., Currie, K.L., and Chappell, B.W., 1987. A-type granites geoehemical, charcteritics, discrimination and petrogenesis. *Contributions to Mineralogy and Petrology*, 95: 407–419.

Wickham, S.M., Alberts, A.D., Litvinovsky, B.A., Bindeman, I.N., and Schauble, E.A. 1996. A stable isotope study of anorogenic magmatism in East Central Asia. *J. Petrol.*, 37: 1063–1095.

Wu Fu-yuan, Sun Deyou, Li Huimin, Jahn, B.M. and Wilde, S., 2002. A-type granites in northeastern China: Age and geochemical constraints on their petrogenesis. *Chem Geol.*, 187: 143–173.

Wu Suoping, Wang Meiying and Qi Kaijing, 2007. Present situation of researches on A-type granites: a review. *Acta Petrologica et Mineralogica*, 26(1): 57–66 (in Chinese with English abstract).

Wu Yuanbao and Zheng Yongfei, 2004. Mineral-genesis of zircon and its constraint to the explain of U-Pb ages. *Chinese Science Bulletin*, 49(16): 1589–1604 (in Chinese).

Xia Qinlin, Chen Yongqing, Lu Yingxiang, Jiang Chengxing, Liu Hongguang and Lǚ Zicheng, 2005. Geochemistry, Fluid inclusion, and stable isotope studies of Luziyuan Pb-Zn deposit in Yunnan Province, Southwestern China. *Earth Science-Journal of China University of Geosciences*, 30(2): 177–186 (in Chinese with English abstract).

Yang Tiannan, Li Jinyi, Sun Guihua and Wang Yanbin, 2008. Mesoproterozoic continental arc type granite in the central Tianshan mountains: zircon SHRIMP U-Pb dating and geochemical analyses. *Acta Geologica Sinica* (English edition), 82(1): 117–125.

Yao Jianxin, Wang Naiwen, Xiao Xuchang, Ji Zhansheng, Wu Guichun, Wu Zhenjie, Li Boqin, Wang Jun, Wang Yong and Zhai Qingguo, 2009. Distribution of the Permian Monodiexodina in Karakorum and Kunlun and its geological significance. *Acta Geologica Sinica* (English edition), 83(2): 229–237.

Yu Saiying, Li Kunqiong, Shi Yuping and Zhang Huihua, 2003. A study on the granodiorite in the middle part of Lincang granite batholith. *Yunnan Geology*, 22(4): 426–442(in Chinese with English abstract).

Yunnan Bureau of Geological Survey, 2006. *Investigative report the great difficulty in exploring in southern Sanjiang region.* Kunming: Yunnan Bureau of Geological Survey (unpublished, in Chinese).

Yuan, H.L., Gao, S., Liu, X.M., Li, H.M., Gunther, D., and Wu, F.Y., 2004. Accurate U-Pb age and trace element determinations of zircon by laser ablation-inductively coupled plasma mass spectrometry. *Geostandards Newsletter*, 28: 353–370.

Zhang Caihua, Liu Jishun and Liu Deli, 2006. Geological and geochemical characteristics and tectonic setting of Triassic volcanic suite in Guanfang area along South Lancangjiang belt. *Acta Petrologica et Mineralogica*, 25(5): 377–386 (in Chinese with English abstract).

Zhao Zhifang, Lu Yingxiang, Xie Yunhong and Li Wenchang. 2002. An example study of remote sensing & GIS metallogenetic prognosis in Luziyuan area, Zhenkang. *Yunnan Geology*, 21(3): 300–307 (in Chinese with English abstract).

Zhong Dalai, 1998. *Paleotethysides in Western Yunnan and Sichuan*. Beijing: Science Publishing House, 1–231 (in Chinese).

Zhu Yuyin, Han Runsheng, Xue Chuandong, Lu Shenlin, Zou Haijun and Yuan Zhihong, 2006. Geological character of the Hetaoping Lead-Zinc deposit of Baoshan, Yunnan Province. *Mineral Resources and Geology*, 20(1): 32–35 (in Chinese with English abstract).